Plasmonic Nanoparticle Aggregates in High-Intensity Laser Fields: Effect of Pulse Duration

Article *in* Plasmonics · August 2015

DOI: 10.1007/s11468-015-0054-8

3 authors, including:

Alexander Ershov
Institute of Computational Modelling
8 PUBLICATIONS **17** CITATIONS
SEE PROFILE

Sergey Karpov
Russian Academy of Sciences
69 PUBLICATIONS **364** CITATIONS
SEE PROFILE

Plasmonics (2016) 11:403–410
DOI 10.1007/s11468-015-0054-8

Plasmonic Nanoparticle Aggregates in High-Intensity Laser Fields: Effect of Pulse Duration

A. E. Ershov[2,3,4] · **A. P. Gavrilyuk**[2,4] · **S. V. Karpov**[1,3,4]

Received: 22 June 2015 / Accepted: 4 August 2015 / Published online: 25 August 2015

Abstract We use an optodynamic model to study the interaction of pulsed laser radiation of different duration with mono- and polydisperse dimers and trimers of plasmonic nanoparticles as resonant domains of colloid Ag multiparticle aggregates. A comparative analysis of the influence of pulse duration on the kinetic characteristics of domains accompanied by the change in their local structure was carried out taking into account the intensity of incident radiation. The obtained results explain the reasons for laser photochromic reactions in materials containing colloidal aggregates of plasmonic nanoparticles.

Keywords Nanoparticle · Surface plasmon · Colloidal aggregate · Optodynamics

Introduction

Processes of interaction of pulsed laser radiation with plasmonic nanoparticles and their aggregates of different configurations is an important field of research in nanoplasmonics. Its significant application potential has been reported in many recent monographs and review papers [1–5].

In particular, these publications cover fabrication of surface plasmon-polariton waveguides and devices, novel solutions in medicine, lab-on-a-chip plasmonic biosensing, plasmonic enhancement of optical properties of metal nanoparticles and ultrasensitive Raman spectroscopy of biomolecules adsorbed by nanoparticles in colloidal aggregates, new nonlinear optical and photochromic composite materials containing plasmonic colloidal aggregates, and so forth. Most the problems require deep understanding of the processes underlying the interaction of high intensity optical radiation with systems of bound plasmonic nanoparticles.

In our papers [6–8], we proposed a model of optodynamic phenomena in colloidal aggregates consisting of bound metal particles exposed to laser pulses of picosecond duration. These phenomena determine the optical feedback of nanocomposite materials and nanocolloids under the action of pulsed laser radiation.

One of the important factors affecting physical processes in laser fields is the duration of exposure of particles in colloidal aggregates to optical radiation. Such optodynamic processes may be accompanied by both an irreversible shift of neighboring nanoparticles in resonant domains and deterioration of the resonance properties of nanoparticles because of heating and melting thereof.

Note that a large number of experiments on nonlinear refraction and nonlinear absorption in nanocolloids of noble metals were carried out with nanosecond and picosecond laser pulses for the same wavelengths [9, 10]. It was found that these experimental results were very different. In particular, the nonlinear refractive index in picosecond pulses was much lower than in nanosecond pulses despite high radiation intensity [10].

PACS: 78.67.Sc; 73.20.Mf

✉ S. V. Karpov
karpov@iph.krasn.ru

[1] L.V. Kirensky Institute of Physics of the RussianAcademy of Sciences, Krasnoyarsk, Russia 660036

[2] Institute of Computational Modeling, Russian Academy of Sciences, Krasnoyarsk, Russia 660036

[3] Siberian state Aerospace University, Krasnoyarsk, Russia 660014

[4] Siberian Federal University, Krasnoyarsk, Russia 660028

In the experiments on laser-induced photochromic processes in Ag nanocolloids occurring near the laser radiation frequency, we observed the effect of spectral- and polarization-selective transparency with formation of a spectrally selective dip [11–13] in the inhomogeneously broadened plasmon absorption spectrum of the Ag nanoparticle aggregate [14]. Moreover, the spectral dips formed by picosecond and nanosecond pulses had a different sign of shift relative to the laser wavelength [12]. These results required explanation, which was impossible without a new physical model.

Our work has been motivated by the absence of explanation for a large volume of experimental data on interaction of laser pulses with plasmonic nanomaterials obtained over the past decade as well as by the new challenges associated with the use of periodic structures in the form of plasmonic nanoparticle chains to waveguide modulated optical radiation of various duration.

The aim of our work is to answer the question how the physics of interaction of laser pulses with simple resonant domains of multiparticle colloidal aggregates (in the form of nanoparticle dimers and trimers of arbitrary particle size) is affected by the pulse duration (ranging from pico- to microseconds). The interest of this problem is due to the fact that within these times (tens of nanoseconds or longer) domains undergo structural changes (relative shifts of particles) while the pulse is on, unlike picosecond pulses [1] where such changes occur long after the pulse is over.

Note that the study of the processes in resonant domains is both of academic and applied interest because it helps understanding the mechanisms of photomodification of real multiparticle colloidal aggregates.

Model

A description of the model is given in [6, 7]. This model describes the interaction of pulsed optical radiation with a simple resonant domain consisting of several bound metal nanoparticles (as well as with a multiparticle aggregate). The resonant domain of a multiparticle aggregate is a group of closely spaced bound particles in an aggregate whose absorption spectrum maximum coincides with the radiation frequency. In our case, the coincidence with the resonant frequency is determined by the maximum value of light-induced dipole moments of particles in a domain. An important factor affecting the optodynamic processes in a resonance domain and the domain optical characteristics is the local environment of particles in the aggregate [8, 15–18]. We will study several types of resonance domains with different local environment (mono- and polydisperse dimers and trimers, Fig. 1) exposed to laser radiation polarized along the domain axis.

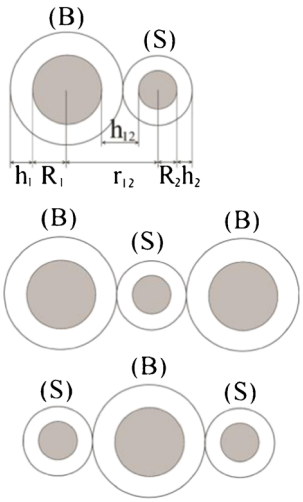

Fig. 1 A schematic drawing of polydisperse domains consisting of particles with adlayers. (*B*)—big and (*S*)—small particle (longitudinal orientation of domain to the laser field polarization)

In accordance with the ideas stated in [6–8], the physical pattern of interaction of a domain with laser radiation is as follows. Before exposure to a laser pulse, the neighboring particles in a domain are in a position of stable equilibrium between the attractive van der Waals and repulsive elastic forces (the latter is due to deformation of the polymer adsorption layer of nanoparticles in the contact area). The high-intensity picosecond laser radiation produces optical interparticle forces, but they act only as long as the pulse is on and do not contribute significantly to photomodification of the domain. In laser pulses of nanosecond duration that can induce photochromic effects as well, the intensity is too low to produce any detectable optical forces. However, absorption of the radiation by the domains leads to heating of the metal core of the particles and to transfer of thermal energy to the polymeric adsorption layer (herein adlayer) resulting in a decreased elasticity modulus of the adlayer. This is accompanied by an imbalance of the acting forces and leads to the collapse of particles in the domain under the van der Waals attraction up to a full contact of their metal surfaces. In turn, the changes in the interparticle gap in the domain after the pulse is over (or during the pulse) are observed as a red shift of the maximum of the domain absorption spectrum with respect to the laser radiation wavelength. This shift explains the static changes in the spectrum persisting after the pulse end. That is, the heating of particles and associated changes in the properties of their adlayer underlie the mechanism determining the position of particles in a domain under applied laser radiation.

Furthermore, we take into account that heating and melting of the particle metal core increase the electron relaxation constant, which reduces the Q-factor of the particle surface plasmon resonance and, hence, changes the interaction of laser radiation with a resonance domain when resonant properties of the system deteriorate. It explains the reason for dynamic spectral changes that manifest themselves only during the pulse action, which is particularly typical of picosecond pulses.

Our model is based on the system of differential equations and the set of linear algebraic equations from [7]:

$$\frac{d\mathbf{r}_i}{dt} = \mathbf{v}_i, \quad i = 1 \ldots N \tag{1}$$

$$m_i \frac{d\mathbf{v}_i}{dt} = (\mathbf{F}_{\mathrm{vdw}})_i + (\mathbf{F}_{\mathrm{el}})_i + (\mathbf{F}_{\mathrm{opt}})_i + (\mathbf{F}_{\mathrm{f}})_i, \tag{2}$$

$$\mathbf{F}_{\mathrm{vdw}} = -\frac{\partial U_{\mathrm{vdw}}}{\partial \mathbf{r}}, \quad \mathbf{F}_{\mathrm{el}} = -\frac{\partial U_{\mathrm{el}}}{\partial \mathbf{r}}, \quad \mathbf{F}_{\mathrm{opt}} = -\frac{\partial U_{\mathrm{opt}}}{\partial \mathbf{r}}, \tag{3}$$

$$\mathrm{U}_{\mathrm{opt}} = -\frac{1}{4}\mathrm{Re}\sum_{i=1}^{N}\left[\mathbf{d}_i \cdot \mathbf{E}^*(\mathbf{r}_i) + \frac{1}{2}\mathbf{d}_i \cdot \left(\frac{\mathbf{d}_i}{\varepsilon_0 \alpha_i} - \mathbf{E}(\mathbf{r}_i)\right)^* - \varepsilon_0 \alpha_i |\mathbf{E}_0|^2\right], \tag{4}$$

$$\mathrm{d}_{i\alpha} = \alpha_i \left[(E_0)_\alpha \exp(i\mathbf{k}\mathbf{r}_i) + \sum_{j \neq i}^{N}\sum_{\beta=1}^{3} G_{\alpha\beta}\left(\mathbf{r}'_{ij}\right)\mathrm{d}_{j\beta}\right], \quad \alpha, \beta = x, y, z, \tag{5}$$

$$\alpha_i = R_i^3 \frac{\varepsilon_i - \varepsilon_{\mathrm{m}}}{\varepsilon_i + 2\varepsilon_{\mathrm{m}} - \frac{2}{3}\mathrm{i}(R_i|\mathbf{k}|)^3(\varepsilon_i - \varepsilon_{\mathrm{m}})} \tag{6}$$

$$\sigma_e = 4\pi|\mathbf{k}|\mathrm{Im}\left[\sum_{i=1}^{N}\frac{\mathbf{d}_i \cdot \mathbf{E}^*(\mathbf{r}_i)}{|\mathbf{E}_0|^2}\right], \quad Q_{\mathrm{e}} = \frac{\sigma_{\mathrm{e}}}{\sum_{i=1}^{N}\pi R_i^2} \tag{7}$$

$$\frac{d(E_{\mathrm{el}})_i}{dt} = -\frac{(E_{\mathrm{el}})_i}{\tau_{\mathrm{r}}((T_{\mathrm{m}})_i)}, \quad r = {}_0\exp\left(\frac{U}{k_B T_m}\right), \tag{8}$$

$$(C_{\mathrm{e}})_i \frac{d(T_{\mathrm{e}})_i}{dt} = -g\left[(T_{\mathrm{e}})_i - (T_{\mathrm{i}})_i\right] + \frac{W_i}{V_i}, \quad W_i = \frac{\omega|\mathbf{d}_i|^2}{2\varepsilon_0}\mathrm{Im}\left(\frac{1}{\alpha_i^*}\right) \tag{9}$$

$$\frac{d(Q_{\mathrm{i}})_i}{dt} = gV_i\left[(T_{\mathrm{e}})_i - (T_{\mathrm{i}})_i\right] + (q_1)_i V_i \tag{10}$$

$$\begin{aligned}(T_{\mathrm{i}})_i = {} & \frac{(Q_{\mathrm{i}})_i}{C_i V_i} H\left((Q_1)_i - (Q_{\mathrm{i}})_i\right) \\ & + \frac{(Q_{\mathrm{i}})_i - (Q_2)_i}{C_i V_i} H\left((Q_1)_i - (Q_{\mathrm{i}})_i\right) \\ & + T_{\mathrm{L}}(R_i) \cdot H\left((Q_1)_i - (Q_{\mathrm{i}})_i\right).\end{aligned} \tag{11}$$

Here, t is the time from the start of the pulse; m_i, R_i, $\mathbf{v}_i$, $\mathbf{r}_i$, $\mathbf{F}_i$ are the mass, radius, speed, and radius vector of the center of mass of the i-th particle and the resultant force; $(\mathbf{F}_{\mathrm{vdw}})$ is the van der Waals force, $(\mathbf{F}_{\mathrm{el}})_i$ is the elastic force related to deformation of the adlayers of contacting particles; $(\mathbf{F}_{\mathrm{opt}})_i$ is the optical force caused by the interaction of light-induced dipoles; $(\mathbf{F}_{\mathrm{v}})_i$ is the viscous friction force; $(\mathbf{F}_{\mathrm{f}})_i$ is the tangential interparticle friction force; $\mathrm{U}_{\mathrm{opt}}$ is the potential energy of interaction of light-induced dipole moments; $\mathbf{d}_i$ is the light-induced dipole moment; $\mathbf{E}(\mathbf{r}_i)$ is the strength of external electromagnetic field ($\mathbf{E}_0$ is the amplitude of field, the symbol (*) denotes complex conjugation); α_i is the dipole polarizability of the i-th particle; τ is the laser pulse duration; $H(x)$ is the Heaviside function; $\mathbf{k}$ is the wave vector of laser radiation; $\mathbf{r}_{ij}$ is the vector joining the centers of the particles, adjusted for the renormalization coefficient [7]; $G_{\alpha\beta}$ is the interparticle interaction tensor; ε_i is the dielectric constant of the particle material taking into consideration its size, temperature, and aggregate state; ε_m is the dielectric constant of the interparticle medium; σ_{e} is the extinction cross section, Q_e is the extinction efficiency, (E_{el}) is the elasticity modulus of particle adlayer; τ_{r} is the relaxation time of molecular bonds in adlayers; $\tau_0 = 10^{-12}$–10^{-13} s is the characteristic vibration period of atoms in molecules; $(T_{\mathrm{m}})_i$ is the average temperature of the heated area near the i-th particle; $(T_{\mathrm{e}})_i$, $(T_{\mathrm{i}})_i$ are the temperatures of electron and lattice (ion) component of the i-th particle; $(C_{\mathrm{e}})_i$ is the volumetric heat capacity of electron components; g is the rate of energy exchange between the electron and ion subsystems; W_i is the absorbed power of laser radiation; V_i is the particle volume; ω is the angular frequency of the laser radiation; $(q_1)_i$ is the heat flow per unit volume describing thermal losses; $T_{\mathrm{L}}(R_i)$ is the size dependence of melting temperature; $(Q_{\mathrm{i}})_i$ is the thermal energy transferred to the ion component of a particle, $(Q_1)_i$, $(Q_2)_i$ are the thermal energies at the initial and final stages of melting. Greek subscripts denote the Cartesian components of vectors and tensors.

In the optodynamic model of interaction of resonant domain with pulsed laser radiation proposed in [6], we took into account a wide range of related thermodynamic, optical, chemical, and mechanical processes. The proposed model reproduces the most realistic pattern of the action of pulsed laser radiation on a resonant domain (compared to the existing optodynamic models [6, 7]) and includes the previously neglected physical processes and phenomena in the models [18–20]. It should be noted that, unlike [6, 7], we use a smaller value of the binding energy in the adlayer U=0.47 eV adjusted based on the experimental data for the elasticity modulus of casein (as the adlayer material). This leads to faster melting of the adlayer at the same temperature.

Results

As in the previous papers [6, 7], the domain characteristics (Figs. 2, 3, 4, and 5) include the parameters in Eqs. (1–11). In contrast to the previous works, changes in the characteristics of domains are studied under the action of pulsed laser radiation with the duration 1000 times longer (τ=20 ns) than in [6, 7] at the wavelength corresponding to the maximum of the extinction (plasmonic) spectrum.

The initial values of the interparticle gap, thickness, and elasticity modulus of the polymer adlayer are $h \approx 1$ nm, $h_i = 0.65$ nm, and $E_{\mathrm{el}} = 3 \cdot 10^8$ N/m^2, respectively ($h < 2h_i$ because of adlayer deformation at the contact area). Particle sizes in the domain and the degree of their polydispersity may be arbitrary.

Our studies were carried out with the domains consisting of both monodisperse and polydisperse nanoparticles: a dimer with the particle radiuses R=8 and 2 nm (configuration "big-

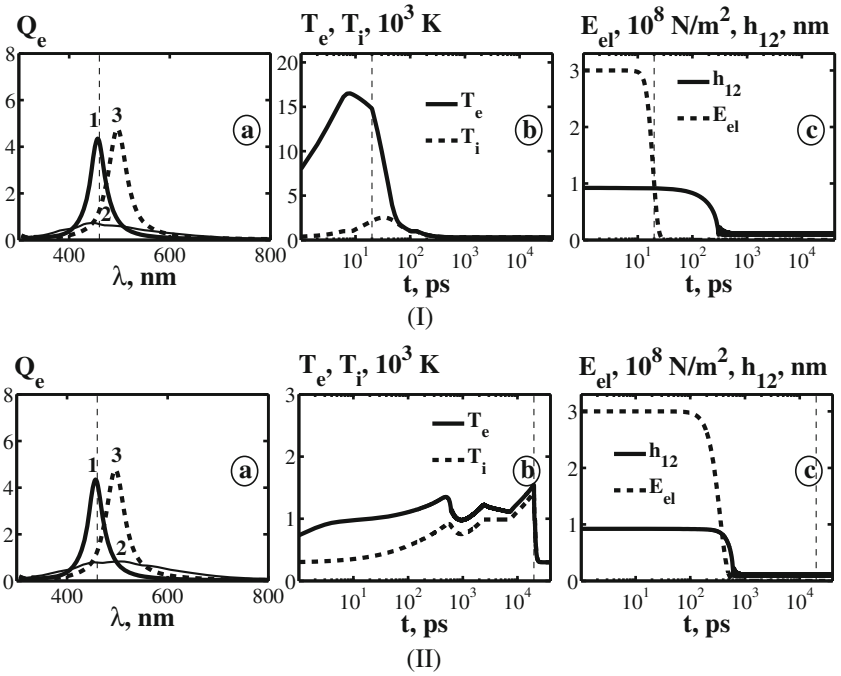

Fig. 2 Comparative kinetics of parameters for the monodisperse dimer (R=5 nm) when exposed to laser pulses (I) is τ=20 ps, (II) is τ=20 ns. The laser wavelength is λ=460 nm, Q_e: *1* is the start (t=0), *2* is at the pulse end (t=20 ps—(I), t=20 ns—(II)), *3* is t=20 ns (I), t=40 ns (II)

small") and a trimer with the particle radius R=2, 8, and 2 nm (configuration "small-big-small") as well as a monodisperse dimer and trimer with a particle radius of 5 nm (which is close to typical experimental values).

Monodisperse Dimer and Trimer

As mentioned above, according to [6, 7], the change in the optical properties of the resonance domain of multiparticle aggregates when it is exposed to a nanosecond laser pulse is caused by two mechanisms: first, the collapse of particles in a domain under the action of the van der Waals attraction and, secondly, the increase in the electron relaxation constant of the particle metal core due to heating and melting of the particle.

The first mechanism is similar to the effects occurring in aggregates exposed to a picosecond pulse. Despite the fact that the intensity of the laser radiation in this case is much lower, the particle adlayer loses its elasticity due to the longer exposure, as it does in high-intensity picosecond pulses. Moreover, an aggregate with its resonant domains has enough time during the pulse to come to a new equilibrium state.

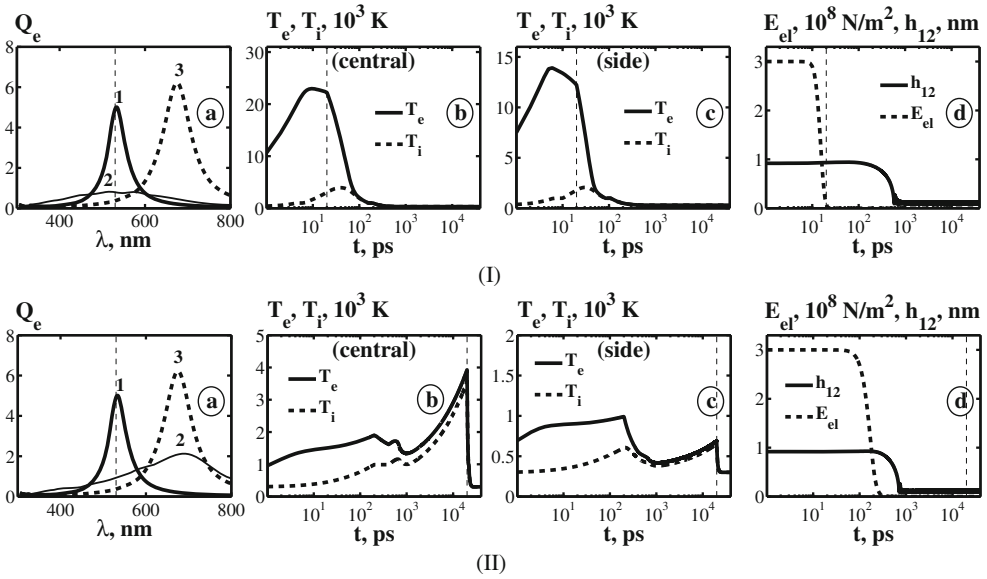

Fig. 3 Comparative kinetics of parameters for the monodisperse trimer (R=5 nm) when exposed to laser pulses with duration (I) τ=20 ps, (II) τ=20 ns. λ=530 nm. Q_e*1*—starting, *2*—at the pulse end (t=20 ps (I), t=20 ns (II)), *3*—t=20 ns (I), t=40 ns (II). Elasticity modulus E_{el} is shown for the central particle. The distance h_{ij} in the trimer corresponds to h_{12} and h_{23}. (I) I=7.5·10^8 W/cm^2, (II) I=8.3·10^6 W/cm^2

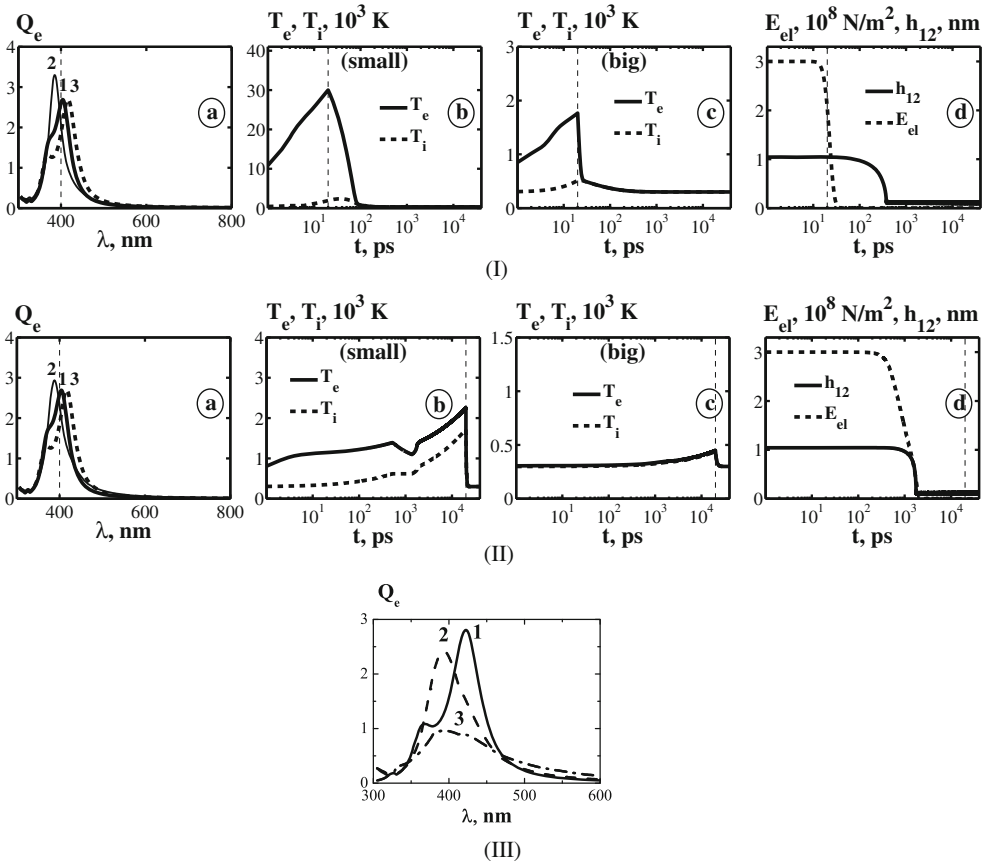

Fig. 4 Comparative kinetics of parameters for a polydisperse dimer (R_S=2 nm, R_B=8 nm) when exposed to laser pulses (*I*) τ=20 ps, (*II*) τ=20 ns. λ=400 nm, Q_e: *1*—the initial stage, *2*—at the pulse end (t=20 ps (*I*), t=20 ns (*II*)), *3*—t=20 ns (*I*), t=40 ns (*II*). The modulus of elasticity is given for the small particle. (*III*)—dynamic evolution of the extinction spectrum of a polydisperse dimer (r_1=2 nm, r_2=7 nm): *1*—the initial spectrum, *2*—2 ps after the pulse beginning (small particles in liquid), *3*—20 ps after the pulse beginning (both particles are liquid). (*I*) I=7.5·10^8 W/cm^2, (*II*) I=8.3·10^6 W/cm^2

The second mechanism may be somewhat different from the processes in a picosecond pulsed field. The melting temperature of particles in resonant domains may not be achieved because of the lower laser intensity. There is only a slight change in the electron relaxation that occurs due to increased electron–phonon interaction rather than destruction of the crystal lattice. Upon reaching the melting point, the dynamic photomodification mechanisms are similar to those observed in picosecond pulses.

Figure 2 shows comparative characteristics of the monodisperse dimer under picosecond (Fig. 2(I)) and nanosecond (Fig. 2(II)) pulses. In all, Figs. 2, 3, 4 and 5 calculations were performed for two radiation intensities: (*I*) I=7.5·10^8 W/cm^2 (for picosecond pulses) and (*II*) I=8.3·10^6 W/cm^2 (for

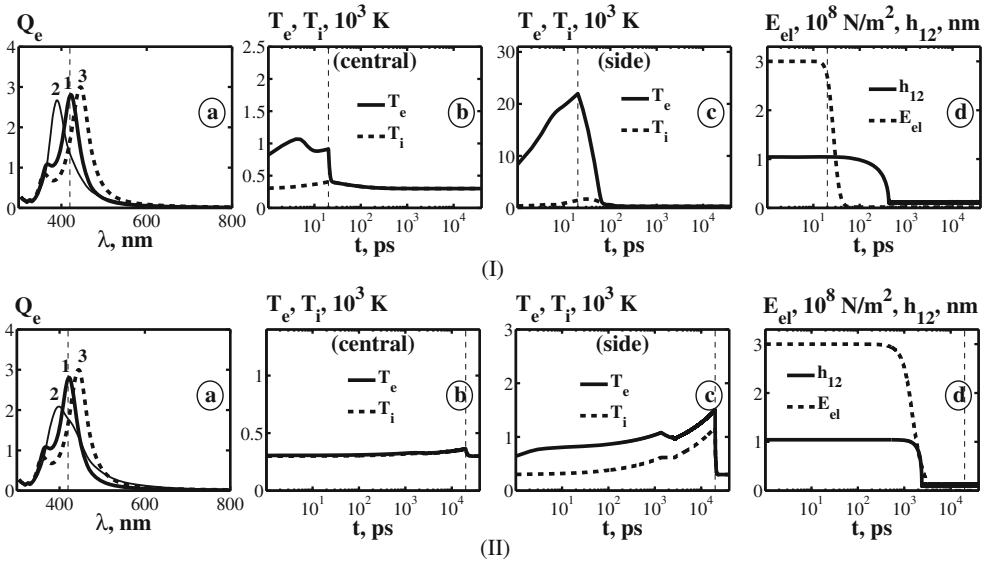

Fig. 5 Comparative kinetics of the parameters of a polydisperse trimer SBS (small—R_s=2 nm, big—R_s=8 nm) when exposed to laser pulses (*I*) τ=20 ps, (*II*) τ=20 ns. λ=420 nm. Q_e: *1*—the initial stage, *2*—at the pulse end (t=20 ps (*I*), t=20 ns (*II*)), *3*—t=20 ns (*I*), t=40 ns (*II*). The elasticity modulus is given for the small particle. (*I*) I=7.5·10^8 W/cm^2, (*II*) I=8.3·10^6 W/cm^2

nanosecond pulses). Photomodification in the case of a nanosecond pulse is distinct in that the threshold radiation intensity causing static changes in the domains is two orders of magnitude lower compared to that for picosecond pulses. At the same time, the required threshold energy density in the latter case is more than an order of magnitude higher. Indeed, in the case of picosecond pulses, a large amount of the absorbed radiation energy is stored in the electron subsystem before the crystal lattice starts melting, and the electron-ion exchange does not have time to occur. But then this energy is transmitted to the ionic lattice anyway. That is, upon melting, the ion subsystem of a particle continues to accumulate energy. When exposed to nanosecond pulses such accumulation of energy in the electron subsystem are too low because of the fast electron-ion exchange and as soon as melting of the particle begins the energy input into the ionic system almost ceases.

Furthermore, the interparticle optical forces are negligibly small for the threshold intensities typical of nanosecond pulses and do not play any significant role in the change of the interparticle distance in a domain. In addition, the temperatures of the electron and ionic components do not substantially differ because of the high rate of heat exchange between these components (Fig. 2(II, b)). Due to the longer pulse duration and accumulation of the optical radiation energy, the process of static modification takes place before the nanosecond pulse is over (Fig. 2(II, c)).

In the case of picosecond pulses, static photomodification during the pulse action does not occur in spite of the temperature of the metallic particle core in this case being significantly higher and the adlayer of the particle losing its elasticity during the pulse. Static photomodification occurs after the pulse is over due to the lag of particles approach. Even after destruction of molecular bonds in the polymer adlayer has occurred and the elastic repulsion of particles significantly weakened, it takes the particles a long time (about 1 ns) to approach each other under the action of the van der Waals forces (Fig. 2(I, c)).

The approach of particles due to the van der Waals forces in a resonant domain during a nanosecond pulse is accompanied by a shift of the maximum in the extinction spectrum to the long-wavelength range (Fig. 2(II, a) curve 3). The dynamic changes, the same as in the case of a picosecond laser pulse, occur due to deterioration of the Q-factor of the surface plasmon resonance (Fig. 2(II, a); curve 2).

Figure 3 illustrates the relative changes in the characteristics describing photomodification of the monodisperse trimer by picosecond (Fig. 3I) and nanosecond (Fig. 3II) laser pulses. Photomodification of domains in the form of trimers (as well as dimers) is distinct in that static changes under applied nanosecond pulses are observed as long as the laser pulse is on. The static changes are attributed to collapse of the resonant domains under the action of the van der Waals forces (Fig. 3(II, d)) and the associated red shift of the maximum in extinction spectrum (Fig. 3(II, a); curve 3) after the pulse end.

Dynamic changes, as in the case of a dimer, are observed as a decrease in the Q-factor (Fig. 3(II, a) curve 2). Eventually, the radiation energy absorbed by particles reduces and the temperature of the particles (Fig. 3(II; b and c)) lowers until it reaches an equilibrium.

The further increase in the temperature (the strong non-monotonicity observed in the time-dependent temperature curves and the presence of veed edges in these curves in Figs. 2(II) and 3(II)) is explained by heating of the particles while heat transfer to the interparticle medium reduces as the temperature of the medium grows. The subsequent cooling of particles (Figs. 2(II) and 3(II, b)) occurs due to their approach and being out of resonance with laser radiation. The resumed temperature rise after cooling in the case of non-resonant heating of a domain is associated with the continued reduction in the heat exchange with the environment.

The reducing Q-factor of the surface plasmon resonance towards the pulse end (Fig. 3(II, a); curve 2—the dynamic photomodification) is associated with melting of the core of the central particle in a trimer (Fig. 3(II, b)). The difference in the heating rates between the central and the side particles in a trimer and the specific behavior of photomodification thereof are attributed to the difference in the local environment and the local fields produced by other particles near the given one [6–8].

In the case of a picosecond pulse, the static photomodification effect during the pulse action is observed neither in a trimer nor in a dimer (Figs. 2(I, c) and 3(I, d)).

Polydisperse Dimer and Trimer

Figures 4 and 5 are a comparative illustration of photomodification of polydisperse domains—a dimer (Fig. 4) and a trimer "small-big-small" (SBS) (Fig. 5) irradiated by of pico- (Figs. 4(I) and 5(I)) and nanosecond (Figs. 4(II) and 5(II)) laser pulses. First of all, note that the extinction spectra of the monodisperse dimers are shifted to longer wavelengths by about 50 nm in dimers and 250 nm in trimers as compared to the polydisperse dimers. As already mentioned [7, 8], a characteristic feature of optodynamic processes in a polydisperse domain is different heating rates for small and large particles as well as a great difference in their temperatures. In this case, photomodification is primarily due to the changes in the properties of the hotter particle.

The process of interaction of a laser pulse with a polydisperse dimer is more complicated. As to the dynamic spectral changes, the small particle in a polydisperse dimer melts first and instead of two resonances in the spectrum (Fig. 4(III, 1)) there remains only one corresponding to the resonance of the big particle (Fig. 4(III, 2)). If the intensity of radiation is high

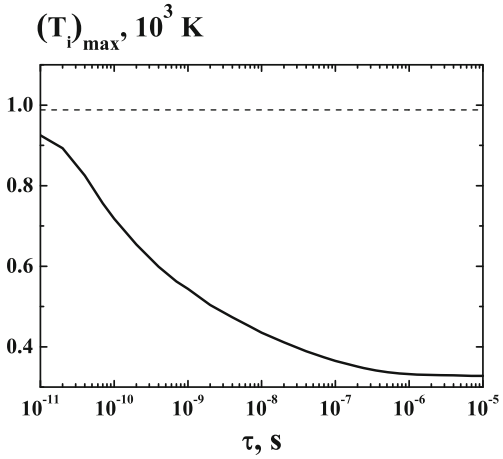

Fig. 6 The maximum ion temperature of monodisperse particles as a function of the pulse duration in the Ag dimer exposed to a laser pulse with a threshold intensity. The *dotted line* shows the melting point of the particles (R=5 nm)

enough the second particle will melt too, which will be evident in the spectrum (Fig. 4(III, 3)).

The essential difference between the process of photomodification of a polydisperse dimer in a laser field of nanosecond duration and photomodification in a picosecond pulse lies in appearance of static changes of the domain characteristics during the pulse action: there is enough time for the adlayer to lose its elasticity and for the particles to shift in the domain within τ. In this case, the extinction spectrum is shifted toward longer wavelengths even before the pulse is over due to collapse of the domain (Fig. 4(II, a); curve 3).

Dynamic photomodification manifests itself in the reduction of the Q-factor of the surface plasmon resonance (Fig. 4(II, a); curve 2) resulting from heating and melting of particles in the domain.

As in the case of monodisperse domains, the temperatures of the electron and ion components of the metallic core almost coincide for nanosecond pulse duration (Fig. 5(II; b and c)), unlike those for picosecond pulses (Fig. 5(I; b and c)).

In Fig. 4(II, b), a sharp drop in the dependence $T_i(t)$ is observed at the moment of collapse (Fig. 4(II, d)). This is due to the increasing influence of the local field of the large particle on the small one. However, the radiation absorption by the large particle drastically decreases as does the local field produced by this particle as soon as the large particle starts melting. This is accompanied by a sharp drop in the temperature of the small particle.

Similar features are observed in photomodification of a polydisperse trimer in nanosecond pulses (Fig. 5(II)). In this case, static changes in photomodification during the pulse are more pronounced (Fig. 5(II, d)). The collapse of a trimer leads to a red shift of the extinction spectrum maximum (Fig. 5(II, a); curve 3). Dynamic changes toward the pulse end are either due to melting of particles and reduction in the Q-factor of the surface plasmon resonance of the particles (Fig. 5(II, a); curve 2) or due to the appearance of an isolated resonance of the big particle when the small ones melt.

Kinetics of the Domain Characteristics in a Wide Range of Pulse Durations

In this section, we study the changes of the characteristics of a monodisperse domain in the form of a Ag dimer under laser radiation in the range of pulse durations from 10^{-11} up to 10^{-5} s.

Figure 6 shows the maximum ionic temperature ($(T_i)_{max}$) of the particle metal core (for the threshold intensities) corresponding static photomodification of the Ag dimer (collapse of the dimer) as a function of the laser pulse duration. The behavior of this curve follows the changes in the kinetics of the elasticity modulus of the particle adlayer. The rate of change of the elasticity modulus depends on the temperature of the ion component of a particle $\left|\frac{dE_{el}}{dt}\right| \sim \exp(-U/k_B T_i)$ [7]. This dependence accounts for the temperature $(T_i)_{max}$ decrease with increasing pulse duration: photomodification in short pulses requires higher temperatures $(T_i)_{max}$ for the elasticity modulus to drop enough to enable static photomodification. The maximum temperature does not exceed the melting temperature of the particles (indicated by dashed line) throughout the pulse duration range.

Figure 7 shows the dependence of the intensity and the energy density of a laser pulse on the pulse duration when the static modification threshold is achieved. In the range τ

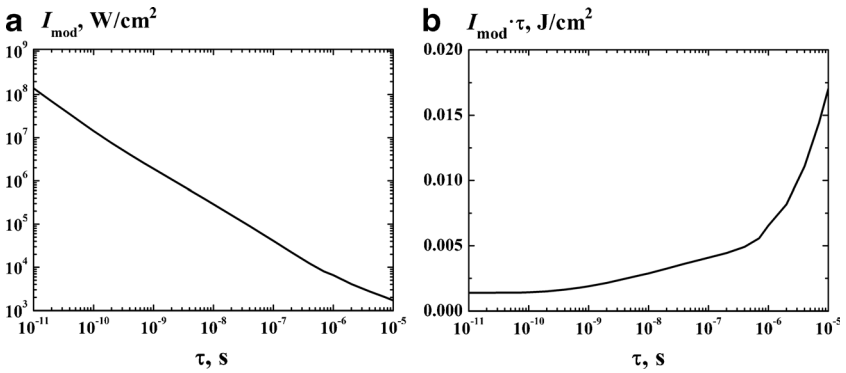

Fig. 7 The dependence of the threshold intensity (**a**) and the radiation energy density (**b**) corresponding to the threshold of static photomodification on the pulse duration

$<10^{-5}$ s, the pulse energy density increases up to its maximum as the pulse duration grows. This is explained by an increase in the energy lost for heat exchange with the environment when τ grows [7], taking into account that the temperature required for photomodification of the domain (Fig. 6) changes inconsiderably (about three times) compared to the change of τ (up to 10^6 times).

Conclusion

The obtained results allow us to answer the question: What is the difference between the impact of a nanosecond laser pulse and a picosecond one on plasmonic nanomaterials containing nanoparticle aggregates?

It has been found that the interparticle forces in the field of optical nanosecond pulses are negligible at the near threshold intensities. Under these conditions both static and dynamic processes occur. The former are due to the collapse of resonant domains of multiparticle aggregates, and the latter are associated with melting of particles in the domains. Both processes are responsible for the changes in the absorption plasmonic spectrum of the domains.

The dynamic changes are associated with the reduction of the Q-factor of the surface plasmon resonance of melted particles. Its manifestation can cover both particles of the domain or be related only to the big particle if the small one is melted.

The temperature of particles in a domain may experience several cycles of increase and decrease during the pulse due to melting of the particles and decrease of the Q-factor of the surface plasmon resonance. Under these conditions, the radiation energy absorbed by the melted particles is reduced.

The temperatures of ionic and electron subsystems in a laser pulse of nanosecond duration are similar.

The minimum threshold radiation intensity in nanosecond pulses is much smaller than that in picosecond pulses due to longer accumulation of the absorbed radiation energy by such a pulse.

Acknowledgments Authors are thankful to Prof. V.A. Markel (University of Pennsylvania) for supplying program codes with realization of coupled dipole method for polydisperse nanoparticle aggregates. This work was performed within the state contract of the RF Ministry of Education and Science for Siberian Federal University for scientific research in 2014 (Reference number 1792)

References

1. Kreibig U, Vollmer M (1995) Optical properties of metal clusters. Springer, Berlin
2. Plasmonics and Plasmonic Metamaterials: Analysis and Applications (2011) Shvets G, Tsukerman I (Editors)(World Scientific Series in Nanoscience and Nanotechnology, Vol. 4)
3. Sarychev AK, Shalaev VM (2007) Electrodynamics of metamaterials. World Scientific Publishing Co. Pte. Ltd, Singapore
4. Sihvola A (2008) Electromagnetic mixing formulas and applications. The Institution of Engineering and Technology Michael Faraday House Six Hills Way, Stevenage Herts, SG1 2AY, United Kingdom
5. Stockman MI (2011) Opt Express 19(22):22030
6. Gavrilyuk AP, Karpov SV (2009) Appl Phys B 97:163
7. Ershov AE, Gavrilyuk AP, Karpov SV, Semina PN (2014) Appl Phys B 115:547
8. Ershov AE, Gavrilyuk AP, Karpov SV, Semina PN (2015) Chin Phys B 24(4):047804
9. Karpov SV, Kodirov MK, Ryasnyanski AI, Slabko VV (2001) Quantum Electron 31:904
10. Ganeev RA, Ryasnyanski AI, Kamalov SR, Kodirov MK, Usmanov TJ (2001) J Phys D Appl Phys 34:1602
11. Karpov SV, Popov AK, Rautian SG, Safonov VP, Slabko VV, Shalaev VM, Shtokman MI (1988) JETP Lett 48(10):571
12. Danilova EY, Rautian SG, Drachev VP, Perminov SV (1996) Bull Russ Acad SciPhys 60:18
13. Safonov P, Shalaev VM, Markel VM, Danilova YE, Lepeshkin NN, Kim W, Rautian SG, Armstrong RL (1998) Phys Rev Lett 80:1102
14. Karpov SV, Basko AL, Popov AK, Slabko VV (2000) Colloid J 62(6):699
15. Karpov SV, Gerasimov VS, Isaev IL, Markel VA (2005) Phys Rev B 72:205425
16. Karpov SV, Gerasimov VS, Isaev IL, Markel VA (2006) J Chem Phys 125:111101
17. Karpov SV, Gerasimov VS, Isaev IL, Podavalova OP, Slabko VV (2007) Colloid J 69(2):159
18. Drachev VP, Perminov SV, Rautian SG, Safonov VP, Khaliullin EN (2002) J Exp Theor Phys 94:901
19. Perminov SV, Drachev VP, Rautian SG (2007) Opt Express 15: 8639
20. Perminov SV, Drachev VP, Rautian SG (2008) Opt Lett 33:2998